

# The nuclear interaction at Oklo 2 billion years ago

Yasunori Fujii

Nihon Fukushi University, Handa, Aichi, 475-0012 Japan

and

Institute of Cosmic Ray Research (ICRR), University of Tokyo,

Tanashi, Tokyo, 188-8502 Japan

Akira Iwamoto, Tokio Fukahori, Toshihiko Ohnuki, Masayuki Nakagawa

Japan Atomic Energy Research Institute (JAERI)

Tokai-mura, Naka-gun, Ibaraki, 319-1195 Japan

Hiroshi Hidaka

Department of Earth and Planetary Systems Science, Hiroshima University

Higashi-Hiroshima, Hiroshima, 739-8526 Japan

Yasuji Oura

Department of Chemistry, Tokyo Metropolitan University,

Hachioji, Tokyo, 192-0397 Japan

Peter Möller

Theoretical Division, Los Alamos National Laboratory, New Mexico 87545, USA

## Abstract

We re-examine Shlyakhter's effort to constrain the time-variability of the coupling constants of the fundamental interactions by studying the anomalous isotopic abundance of  $\text{Sm}$  observed at the remnants of the natural reactors which were in operation at Oklo about 2 billion years ago. We rely on new samples that were carefully collected to minimize natural contamination and also on a careful temperature estimate of the operating reactor. We find that our result almost re-establishes the original conclusion; the upper bounds on the fractional rate of change of the strong and electromagnetic interaction coupling constants are  $10^{-18}$  {  $10^{-19} \text{ y}^{-1}$  and  $10^{-17} \text{ y}^{-1}$ , respectively. To reinforce the results obtained from  $\text{Sm}$ , we also applied our analysis to  $\text{Gd}$ , for which it was essential to take into account the effect of contamination.

---

A preliminary report is found in Ref. [1].

# 1 Introduction

Few aspects of physics can be understood without recourse to fundamental "constants," such as the speed of light  $c$ , Planck's constant  $h$ , Newton's constant  $G$ , the fine-structure constant  $\alpha$ , and its strong-interaction counterpart  $\alpha_s$ . To this list one may also add the masses of certain fundamental particles, like the quarks and the leptons, or some of the vacuum expectation values, and perhaps the cosmological constant  $\Lambda$ . The traditional assumption that these parameters of physics theories are constant was challenged for the first time by Dirac, who suggested that  $G$  might vary as  $t^{-1}$  with the cosmic time [2]. This paper inspired to many probes of the possible time variability of various fundamental constants.

However, no positive evidence for any time-dependence has been discovered so far, nor does Dirac's original argument seem fully convincing. Nevertheless, the very idea that at least some of the fundamental constants may not be truly constant still attracts serious attention partly because this appears to be a rather general outcome of the recent efforts toward unifying particle physics and gravity.

Quite remarkable is the finding that the upper bounds obtained so far for  $\alpha$  and  $\alpha_s$  are many orders of magnitude below the value  $10^{10} \text{ y}^{-1}$  expected naturally in terms of the present age of the universe  $t_0 \approx 10^{10} \text{ y}$  [3{9]. The same tendency is indicated also for  $G$  [10]. This is expected to provide an important clue to the nature of a model of unification.

The most stringent constraint ever reported is due to Shlyakhter [6,7] who exploited the exceptionally sensitive dependence of the cross section of the reaction



on the energy of a resonance lying as low as  $E_r = 97.3 \text{ meV}$  above threshold, which corresponds to the temperature  $856 \text{ C}$  and is much smaller than any of the mass scales of the strong or the electromagnetic interaction.

It was noticed that the anomalous abundance of  ${}^{149}\text{Sm}$  observed at Oklo [11,12] can be understood rather well in terms of the reaction (1) with the fundamental-constant values observed today. An analysis of the uncertainties in the Oklo observations provides an upper bound on the possible deviation of the neutron-capture cross section  $\sigma_{149}$  associated with the reaction (1) occurring 2 billions years ago from its present value. One obtains that  $j_{149} = \sigma_{149} \lesssim 10\%$ , which implies  $j_{E_r} \lesssim 20 \text{ meV}$ . Furthermore Shlyakhter derived that  $j_{\alpha_s} = \alpha_s \lesssim 5 \cdot 10^{10} \text{ y}^{-1}$ , or  $j_{\Lambda} = \Lambda \lesssim 2.5 \cdot 10^{19} \text{ y}^{-1}$ , which represent upper bounds on the time-variability of the fundamental constants that are several orders of magnitude more stringent than any other estimate of these bounds [3{9].

However, this substantial improvement of the upper-bound estimate does not seem fully appreciated, because complete details of the analysis have never been published. Another reason for the limited acceptance may be that the derivation steps are much less direct than in estimates based on quasi-stellar-object spectra or on clock standards.

The purpose of this paper is to reconstruct Shlyakhter's analysis in full detail and apply it to new data taken from samples selected with much care and with a geologist's expertise so as to limit potential outside contamination as much as possible. The new, refined analysis we undertake here confirms and reinforces the original result.

During course of our investigation we learned that essentially the same approach had been published by Damour and Dyson [13]. However, we have obtained somewhat stronger upper bounds than in Ref. [13]. Their less stringent bounds were obtained because they relied on earlier data, which we suspect to be seriously affected by contamination. We also point out that their bounds could have been somewhat more stringent if they had not made unnecessarily generous choices of some of their criteria. Although we naturally find some of our formalism is identical to that of Ref. [13], we present here sufficient background material to make our presentation self-contained.

Since also  $^{155}\text{Gd}$  and  $^{157}\text{Gd}$  have low-lying resonances, we expect that also here a study of the neutron-capture reaction products will permit a stringent estimate of upper bounds on the time-variability of the fundamental constants. Unfortunately, the absorption effect is more significant than in  $^{149}\text{Sm}$ , which results in much smaller abundances. Therefore, contamination is a more serious issue here. However, by taking advantage of the presence of these two isotopes we are able to reach a nontrivial result, which corroborates the conclusions obtained from our analysis of the abundances related to the neutron absorption on  $^{149}\text{Sm}$ .

In our investigation below we first introduce the basic equations that are used in our analyses: in Section 2 those related to neutron absorption and in Section 3 those related to nuclide transformations along isotope chains. New measurements on five relatively recent samples are then presented and analyzed in Section 4, providing a better upper-bound on  $E_r$ . Section 5 discusses the relevance of the results to the possible time-variation of the strong-interaction and the electromagnetic-interaction coupling constants. Section 6 gives a summary of the results obtained in our investigation. Appendix A provides some details of the numerical calculation of the thermal average of the resonance cross sections.

## 2 Neutron absorption cross sections

As was mentioned already in Section 1, the results obtained in this investigation are based on an analysis of the neutron-absorption cross section in the reaction (1) and the corresponding reactions on Gd. The reactions are dominated by a resonance, which we describe in the standard Breit-Wigner form,

$$\sigma_r = \frac{g_0}{2mE} \frac{h^2}{(E - E_r)^2 + \frac{\Gamma_{\text{tot}}^2}{4}}; \quad (2)$$

where  $g_0 = (2J + 1) / [(2s + 1)(2I + 1)]$  is the statistical factor,  $s$  the spin of the neutron,  $I$  the spin of the target,  $J$  the spin of the compound nucleus, and where  $\Gamma_{\text{tot}} = \Gamma_n + \Gamma_\gamma$  is the total width in terms of the neutron and the photon widths, respectively. Also,  $\Gamma_n = (2k/K)D$ , where  $k^2 = 2mE = \hbar^2 K^2$ , where  $K$  is the wave number inside the target nucleus, and where  $D$  is the level spacing of the compound levels. The values of these parameters are shown in Table 1 for the lowest-lying resonance in the reactions on  $^{149}\text{Sm}$ ,  $^{155}\text{Gd}$  and  $^{157}\text{Gd}$ .

We now derive how the isotopic abundances observed today depend  $E_r$ , since we need to consider the possibility that  $E_r$  were different from its present value 2 billion years ago. Other parameters may be assumed constant, since only  $E_r$  will affect the result in any

Channel	$^{149}\text{Sm}$	$^{155}\text{Gd}$	$^{157}\text{Gd}$
Resonance energy $E_r$ (meV)	97.3	26.8	31.4
Neutron width $\Gamma_n$ (meV)	0.533	0.104	0.470
Gamma width $\Gamma_\gamma$ (meV)	60.5	108	106
Statistical factor $g_0$	9/16	5/8	5/8

Table 1: Parameters of the lowest-lying resonances used in the present analysis. The tabulated values of  $E_r$  are the present resonance-position values  $E_{r0}$ . The listed values of  $\Gamma_n$  are estimated at  $E_r$ .

significant manner. Note that we would normally expect abundance changes not much larger than  $\delta s = s$ , unless they are amplified by the resonance mechanism and by the extremely small value of  $E_r$  relative to any of the mass scales of nuclear physics.

We average (2) with respect to the thermal neutron flux,

$$\langle \sigma(E; T) \rangle = \langle \sigma(E) \rangle \langle \phi(E; T) \rangle; \quad \text{with} \quad \phi(E) = \frac{v}{2E} \quad (3)$$

where

$$\langle \phi(E; T) \rangle = 2^{-1/2} T^{-3/2} e^{-E/T} \frac{P}{E} \quad (4)$$

is the normalized Maxwell-Boltzmann distribution.

Normally the thermally averaged cross section is defined by

$$\langle \sigma(T) \rangle = \left[ \int_0^\infty \sigma(E) \phi(E; T) dE \right]^{-1} \quad (5)$$

where

$$D(T) = \int_0^\infty \phi(E; T) dE : \quad (6)$$

However, in most of the analyses of the Oklo phenomenon, it is customary [14] to replace the denominator  $D(T)$  by

$$\hat{D} = v_0 \int_0^\infty \phi(E; T) dE = v_0; \quad (7)$$

for a convenient choice of the velocity  $v_0 = 2200$  (m/s) corresponding to the temperature  $T_0 = (m/2k)v_0^2 = 20.4$  C, hence defining an effective cross section

$$\hat{\sigma}(T) = \hat{D}^{-1} \int_0^\infty \sigma(E) \phi(E; T) dE = \frac{\int_0^\infty \sigma(E) \phi(E; T) dE}{\int_0^\infty \phi(E; T) dE} \quad (8)$$

The advantage of this non-standard definition is that, unlike  $D(T)$ ,  $\hat{D}$  is a constant, independent of  $T$ . We note that the neutron flux at Oklo 2 billion years ago is determined based on the observed abundances of  $^{143,145}\text{Nd}$  and  $^{147}\text{Sm}$ . The corresponding neutron absorption cross sections are known to obey a  $1/v$  behavior to a good approximation,

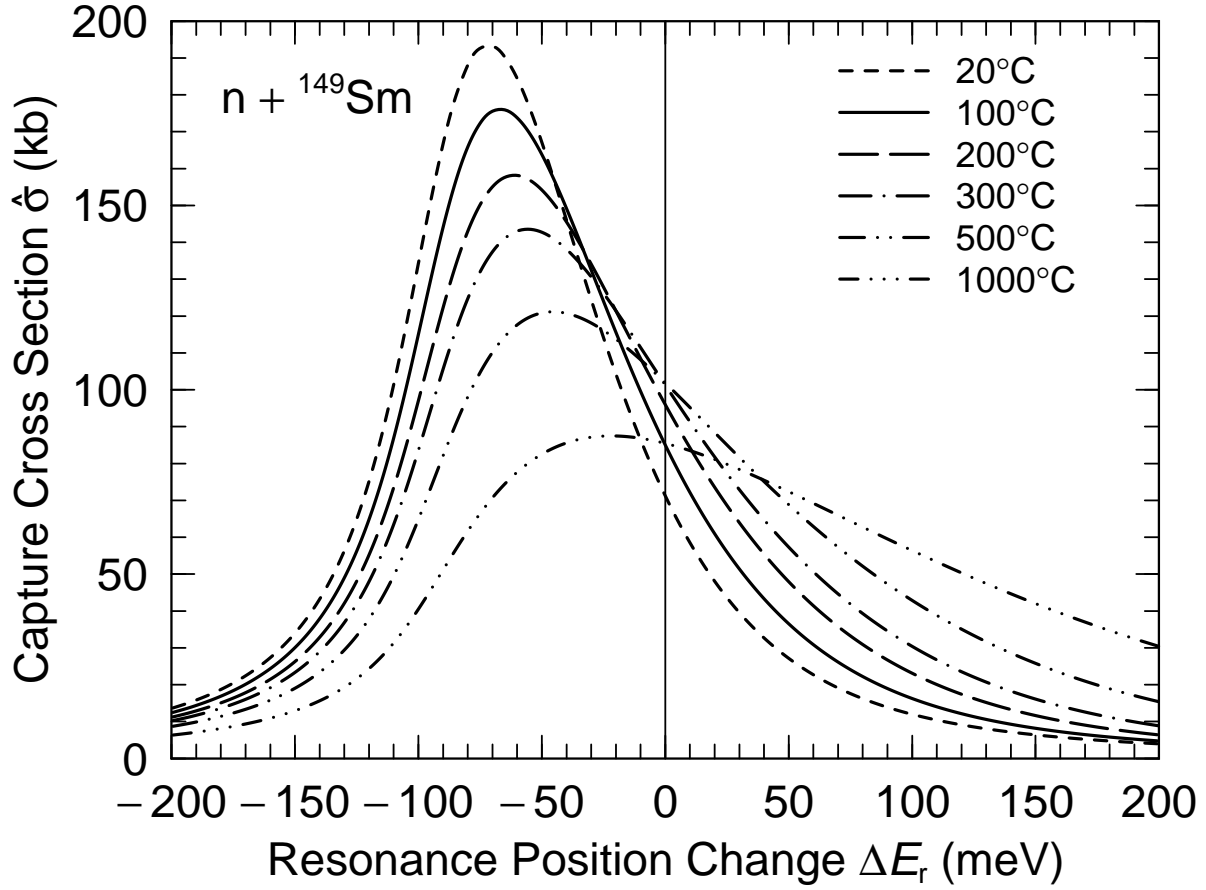


Figure 1: Calculated thermally averaged cross sections  $\hat{\sigma}_{149}$  for  $n + {}^{149}\text{Sm} \rightarrow {}^{150}\text{Sm} + \gamma$  as functions of the resonance position change  $\Delta E_r$  and the temperature  $T$ .

implying that the effective cross sections of these processes are nearly  $T$ -independent, hence simplifying the practical analysis considerably.

In the following analysis, the cross sections always occur multiplied by the thermally averaged flux  $\phi(T)$ . It is obviously convenient to introduce an effective flux  $\hat{\phi}$  in such a way that the product with  $\hat{\sigma}$  remains the same as the original product:

$$\hat{\sigma} \phi = \hat{\sigma} \hat{\phi} \quad (9)$$

Using the last expression of (8), we find

$$\hat{\phi} = \frac{\phi_0}{4T} \quad (10)$$

We evaluate the integral in (8) by numerical integration. Details of the calculation are found in Appendix A. The results for reactions on  ${}^{149}\text{Sm}$ ,  ${}^{155}\text{Gd}$ , and  ${}^{157}\text{Gd}$  are shown in Figs. 1-3, respectively. The figures illustrate the strong dependence of the thermally-averaged cross section on the resonance-position change  $\Delta E_r$  for various reactor temperatures  $T$ .

We have calculated numerically the effect of thermal fluctuations of the atoms in the neutron absorber on the calculated cross sections. The magnitude of this so-called

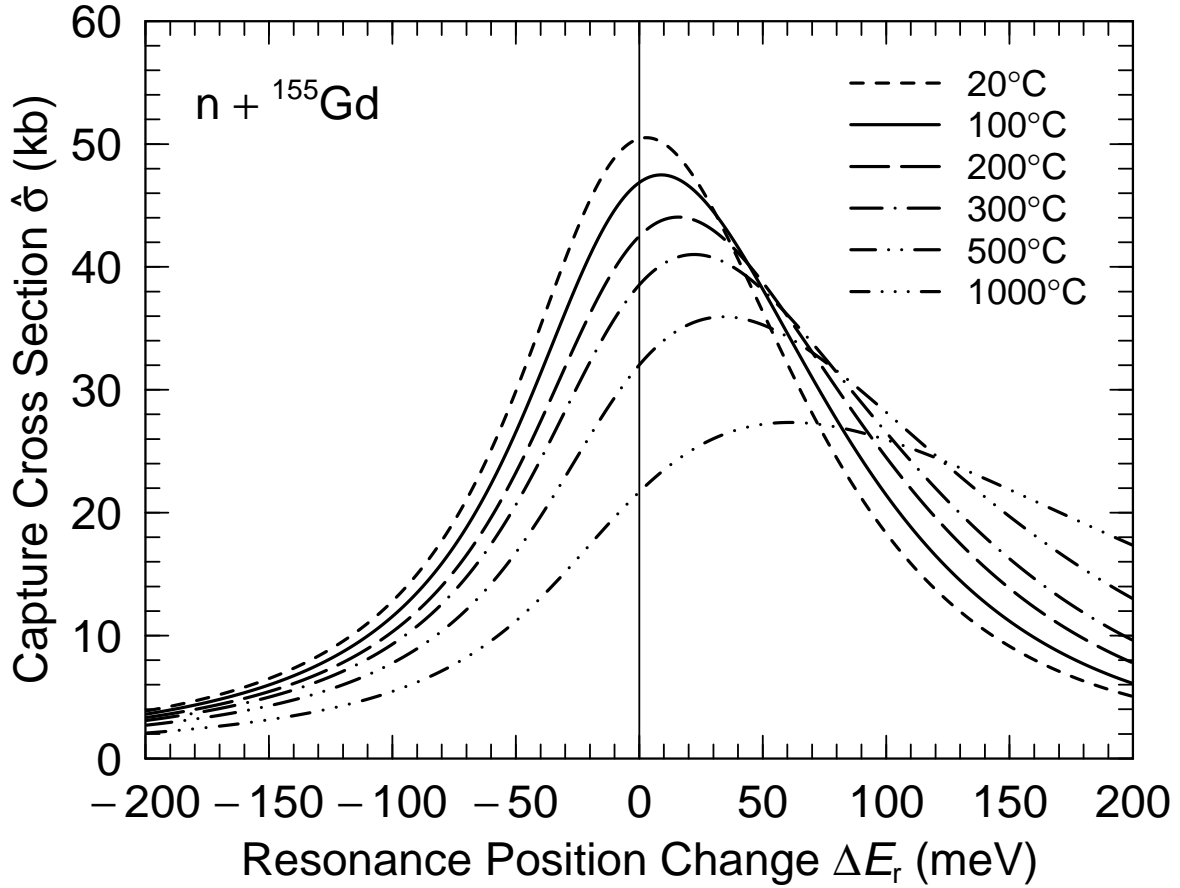


Figure 2: Calculated thermally averaged cross sections  $\hat{\sigma}_{155}$  for  $n + {}^{155}\text{Gd} \rightarrow {}^{156}\text{Gd} + \gamma$  as functions of the resonance position change  $\Delta E_r$  and the temperature  $T$ .

Doppler effect on the calculated  $\hat{\sigma}(T)$  is less than 1% even at the highest temperature investigated, 1000 C, and much smaller for lower temperatures. Therefore this effect can be safely ignored, and the formalism below is for simplicity developed without including Doppler broadening.

### 3 Relations for isotopic compositions

The isotope ratios present in Oklo today are superpositions of contributions from fission, subsequent neutron capture, and of the original natural abundances. The interpretation of the observed abundances is simplified when in special cases some processes do not contribute. In a few of those cases, where the various contributions to the now observed isotope ratios are most easily disentangled, we may draw stringent conclusions about the variation in time of a few low-lying neutron-resonance positions. We consider here the cases of neutron capture on  ${}^{149}\text{Sm}$ ,  ${}^{155}\text{Gd}$ , and  ${}^{157}\text{Gd}$ .

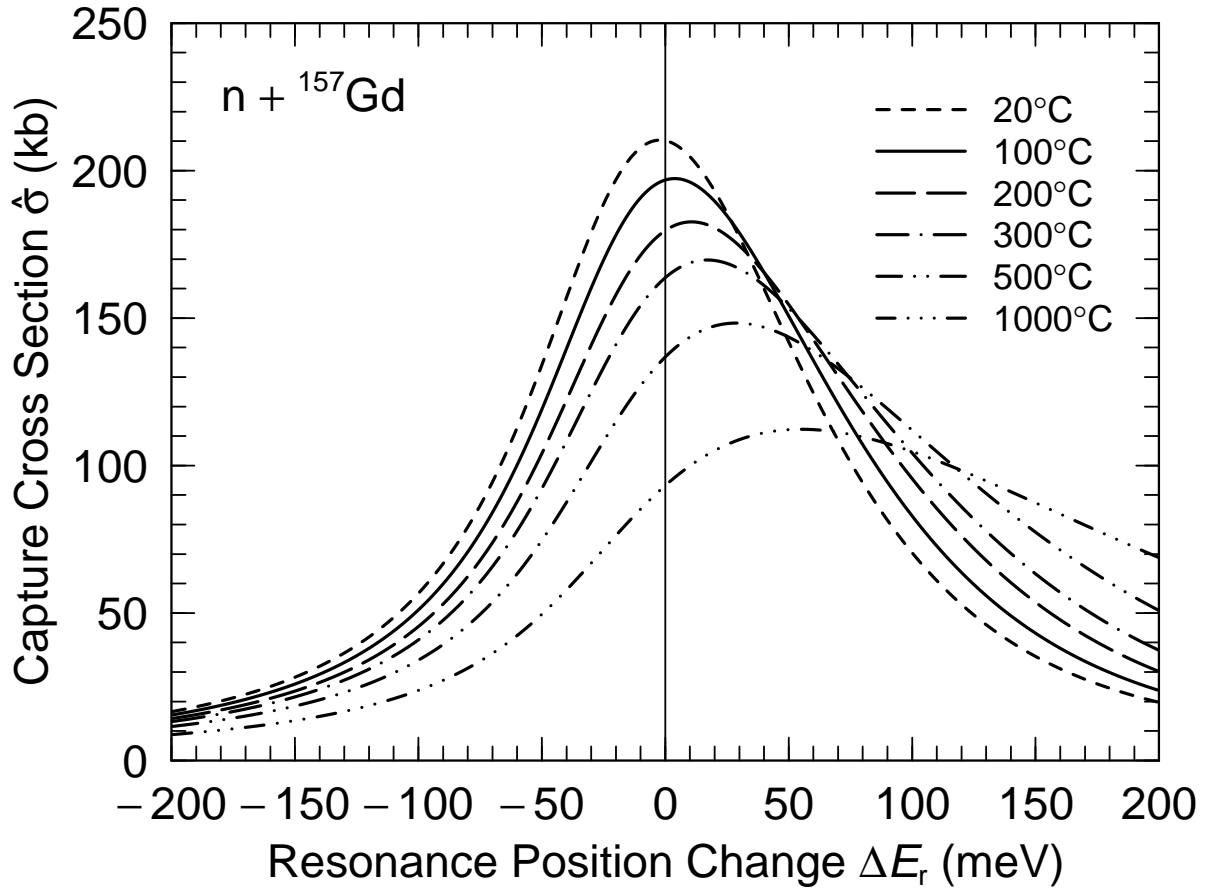


Figure 3: Calculated thermally averaged cross sections  $\hat{\sigma}_{157}$  for  $n + {}^{157}\text{Gd} \rightarrow {}^{158}\text{Gd} + \gamma$  as functions of the resonance position change  $\Delta E_r$  and the temperature  $T$ .

### 3.1 Isotopic composition of Sm

We can make a few observations that simplify the differential equations obtained for the time evolution of the number of atoms per unit volume  $N_A(t)$  of the samarium isotopes  ${}^A\text{Sm}$  near  ${}^{149}\text{Sm}$  that are connected by nuclear transformations. The spontaneous fission half-lives of  ${}^{235}\text{U}$  and  ${}^{238}\text{U}$  exceed  $10^{16}$  y. Therefore fission products are generated in appreciable amounts only by neutron-induced fission during the period of operation of the natural reactors at Oklo. Some isotopes are shielded by stable nuclides and cannot be reached in the  $\beta$ -decay of the unstable nuclei created during the fission process. In addition, it is possible to neglect some neutron-capture reactions, for example capture on  ${}^{148}\text{Sm}$ , because of their low cross sections.

Thus, we obtain the following differential equations:

$$\begin{aligned}
 \frac{dN_{147}(t)}{dt} &= \hat{\sigma}_{147} N_{147}(t) + N_{235}^0 \exp(-\hat{\sigma}_f t) \hat{\gamma}_{147}; \\
 \frac{dN_{148}(t)}{dt} &= \hat{\sigma}_{147} N_{147}(t); \\
 \frac{dN_{149}(t)}{dt} &= \hat{\sigma}_{149} N_{149}(t) + N_{235}^0 \exp(-\hat{\sigma}_f t) \hat{\gamma}_{149};
 \end{aligned} \tag{11}$$

where  $\hat{\sigma}_f$  is the neutron-induced fission cross section of  $^{235}\text{U}$ ,  $Y_{147}$  and  $Y_{149}$  are the fission yields of  $^{147}\text{Sm}$  and  $^{149}\text{Sm}$ , respectively, and  $\hat{\sigma}_f$  the effective flux defined in Eq. (10). The fission cross section  $\hat{\sigma}_f$  is not the bare fission cross section but an effective cross section which includes the restitution of  $^{235}\text{U}$ . Restitution refers to the sequence of events in which a neutron is captured by  $^{238}\text{U}$  and  $^{235}\text{U}$  is the final decay product created via two  $\beta$ -decays yielding  $^{239}\text{Pu}$  and a subsequent  $\alpha$  decay. The time  $t$  starts at the beginning of the reactor period, with  $\hat{\sigma}_f$  assumed to be constant in time. Obviously  $\hat{\sigma}_{149}$  is dominated by the thermally averaged cross section of the absorption process (1) while  $\hat{\sigma}_{147}$  is the non-resonant absorption cross section of  $^{147}\text{Sm}$ .

The initial number densities  $N_A(0)$  are  $N_{235}^0$  for  $^{235}\text{U}$  and

$$N_A(0) = N_A^{\text{nat}} R_A^{\text{nat}}; \quad (12)$$

for the samarium isotopes, for which the relative fractional natural abundances  $R_A^{\text{nat}}$  have been observed to be

$$R_{144}^{\text{nat}} = 0.0310; \quad R_{147}^{\text{nat}} = 0.1500; \quad R_{148}^{\text{nat}} = 0.1130; \quad \text{and} \quad R_{149}^{\text{nat}} = 0.1380; \quad (13)$$

The value for the stable and inactive  $^{144}\text{Sm}$  is included, because it is needed later, whereas the final results will be independent of the overall normalization constant  $N^{\text{nat}}$  and the capture cross section  $\hat{\sigma}_{147}$ .

The solution of the system of differential equations (11) is:

$$\begin{aligned} N_{149}(t) &= \frac{N_{235}^0 \hat{\sigma}_f Y_{149}}{\hat{\sigma}_f \hat{\sigma}_{149}} \exp(-\hat{\sigma}_{149} \hat{\phi} t) \exp(-\hat{\sigma}_f \hat{\phi} t) + N^{\text{nat}} R_{149}^{\text{nat}} \exp(-\hat{\sigma}_f \hat{\phi} t); \\ N_{147}(t) + N_{148}(t) &= N_{235}^0 Y_{147} \frac{1}{\hat{\sigma}_f} \exp(-\hat{\sigma}_f \hat{\phi} t) + N^{\text{nat}} (R_{147}^{\text{nat}} + R_{148}^{\text{nat}}); \end{aligned} \quad (14)$$

from which it follows that

$$\begin{aligned} \frac{N_{147}(t_1) + N_{148}(t_1)}{N_{149}(t_1)} &= \frac{k Y_{147} \frac{1}{\hat{\sigma}_f} \exp(-\hat{\sigma}_f \hat{\phi} t_1) + (R_{147}^{\text{nat}} + R_{148}^{\text{nat}})}{\frac{k \hat{\sigma}_f Y_{149}}{\hat{\sigma}_f \hat{\sigma}_{149}} \exp(-\hat{\sigma}_{149} \hat{\phi} t_1) \exp(-\hat{\sigma}_f \hat{\phi} t_1) + R_{149}^{\text{nat}} \exp(-\hat{\sigma}_f \hat{\phi} t_1)}; \end{aligned} \quad (15)$$

at  $t_1$ , the end of the reactor activity. Since then the samarium isotope concentrations  $N_A(t)$  have remained unchanged until today, unless corresponding, naturally-occurring isotopes have flowed into the sample regions from the outside.

The ratio  $k \frac{N_{235}^0}{N_{235}} = N^{\text{nat}}$  can be determined in the following way. We observe that  $^{144}\text{Sm}$  is never produced as a fission product and has a negligible capture cross section for neutron capture, that is  $N_{144}(t)$  is constant. We may then calculate the ratio  $N_{144}(t_1) = (N_{147}(t_1) + N_{148}(t_1))$  and compare to the observed ratio:

$$\begin{aligned} & \frac{N_{144}(t_1)}{N_{147}(t_1) + N_{148}(t_1)} \quad \text{Observed} \quad R_0 \\ & \frac{N_{144}(t_1)}{N_{147}(t_1) + N_{148}(t_1)} \quad \text{Calculated} \quad = \end{aligned}$$

	Sample				
	SF 84-1469	SF 84-1480	SF 84-1485	SF 84-1492	SD 37
$\hat{t}_1$ (1/kb)	0.525	0.798	0.622	0.564	0.780
$N_{144}(t_1)$ (%)	0.1052	0.2401	0.2073	0.1619	0.06909
$N_{147}(t_1)$ (%)	55.34	53.23	54.03	54.81	52.74
$N_{148}(t_1)$ (%)	2.796	3.468	3.079	2.890	4.694
$N_{149}(t_1)$ (%)	0.5544	0.2821	0.4466	0.4296	0.3088
$N_{235}^0(t_1)=^{238}\text{U}$	0.03181	0.02665	0.02971	0.03047	0.02435
$\hat{\sigma}_{149}$ (kb)	85.6	96.5	83.8	99.0	89.5

Table 2: Measured isotopic ratios and fluences for Sm for five samples and corresponding, calculated values of the cross section  $\hat{\sigma}_{149}$ .

$$\frac{N_{144}^{\text{nat}} R_{144}^{\text{nat}}}{N_{235}^0 Y_{147} [1 - \exp(-\hat{\sigma}_f t_1)] + N^{\text{nat}} (R_{147}^{\text{nat}} + R_{148}^{\text{nat}})} = \frac{R_{144}^{\text{nat}}}{k Y_{147} [1 - \exp(-\hat{\sigma}_f t_1)] + (R_{147}^{\text{nat}} + R_{148}^{\text{nat}})} : \quad (16)$$

From these equations, we obtain

$$k = \frac{R_{144}^{\text{nat}} - R_0 (R_{147}^{\text{nat}} + R_{148}^{\text{nat}})}{R_0 Y_{147} [1 - \exp(-\hat{\sigma}_f t_1)]} : \quad (17)$$

which can be estimated from the observed values only.

We finally solve (15) for  $\hat{\sigma}_{149}$  by using observed abundances and the fluence ( $\hat{t}_1$ ) defined earlier. The results for five recently analyzed samples are shown in Table 2 [15].

### 3.2 Isotopic composition of Gd

For gadolinium we may define relative fractional natural abundances  $R_A^{\text{nat}}$  in complete analogy with samarium in Eq. (12). For Gd the relative fractional natural abundances for the relevant isotopes are

$$\begin{aligned} R_{155}^{\text{nat}} &= 0.1480; & R_{156}^{\text{nat}} &= 0.2047; & R_{157}^{\text{nat}} &= 0.1565; \\ R_{158}^{\text{nat}} &= 0.2484; & \text{and } R_{160}^{\text{nat}} &= 0.2186; \end{aligned} \quad (18)$$

Because  $^{160}\text{Gd}$  is almost stable and inactive, we can use the value of the nearly constant  $N_{160}(t)$  observed at each sample location to determine  $N^{\text{nat}}$ .

Because the neutron-absorption cross sections  $\hat{\sigma}_{156}$  and  $\hat{\sigma}_{158}$  are very small and because  $^{154}\text{Gd}$  is shielded by the stable  $^{154}\text{Sm}$  the study of the possible shifts of the low-lying resonances in  $^{155}\text{Gd}$  and  $^{157}\text{Gd}$  is considerably simplified: we may study the transmutations

related to the isotope pairs  $^{155}\text{Gd}\{^{156}\text{Gd}$  and  $^{157}\text{Gd}\{^{158}\text{Gd}$  separately. The differential equations for the number of atoms  $N_A(t)$  per unit volume for the first isotope pair are:

$$\begin{aligned}\frac{dN_{155}(t)}{dt} &= -\lambda_{155} N_{155}(t) + N_{235}^0 \exp(-\lambda_f t) \lambda_f Y_{155}; \\ \frac{dN_{156}(t)}{dt} &= \lambda_{155} N_{155}(t) + N_{235}^0 \exp(-\lambda_f t) \lambda_f Y_{156};\end{aligned}\quad (19)$$

where we ignored the small cross section  $\lambda_{156}$ . We find the solution:

$$\begin{aligned}N_{155}(t) &= \frac{N_{235}^0 \lambda_f Y_{155}}{\lambda_f - \lambda_{155}} \exp(-\lambda_{155} t) \exp(-\lambda_f t) \\ &\quad + N_{155}^{\text{nat}} \exp(-\lambda_{155} t); \\ N_{155}(t) + N_{156}(t) &= N_{235}^0 (Y_{155} + Y_{156}) \frac{1}{\lambda_f} \exp(-\lambda_f t) \\ &\quad + N_{155}^{\text{nat}} + N_{156}^{\text{nat}};\end{aligned}\quad (20)$$

Also corresponding to (16) we introduce

$$R_0 = \frac{N_{160}(t_1)}{N_{155}(t_1) + N_{156}(t_1)};\quad (21)$$

which can be compared with the observed data expressed in terms of  $N_{160} \Rightarrow N_{156}$  and  $N_{155} \Rightarrow N_{156}$  with reference to the stable isotope  $^{160}\text{Gd}$ . The ratio  $k = \frac{N_{160}^0}{N_{235}^0} \Rightarrow \frac{N_{156}^{\text{nat}}}{N_{155}^{\text{nat}}}$  is given analogously to (17) by

$$k = \frac{R_{160}^{\text{nat}}}{R_0} \frac{(R_{155}^{\text{nat}} + R_{156}^{\text{nat}})}{\lambda_f - \lambda_{155}} \exp(-\lambda_f t_1);\quad (22)$$

Now  $\lambda_{155}$  can be determined by solving iteratively

$$\frac{N_{155}(t_1)}{N_{156}(t_1)} = \frac{A}{B};\quad (23)$$

where the observed ratio is substituted into the left-hand side, and where

$$\begin{aligned}A &= \frac{k \lambda_f Y_{155}}{\lambda_f - \lambda_{155}} \exp(-\lambda_{155} t_1) \exp(-\lambda_f t_1) + N_{155}^{\text{nat}} \exp(-\lambda_{155} t_1); \\ B &= \frac{k Y_{155}}{\lambda_{155} - \lambda_f} \frac{1}{\lambda_{155}} \exp(-\lambda_f t_1) \frac{1}{\lambda_f} \exp(-\lambda_{155} t_1) \\ &\quad + k Y_{156} \frac{1}{\lambda_f} \exp(-\lambda_f t_1) + N_{155}^{\text{nat}} \frac{1}{\lambda_{155}} \exp(-\lambda_{155} t_1) + N_{156}^{\text{nat}};\end{aligned}\quad (24)$$

The transmutation equations related to the isotope pairs  $^{157}\text{Gd}$  and  $^{158}\text{Gd}$  are obtained by replacing quantities related to  $^{155}\text{Gd}$  and  $^{156}\text{Gd}$  by quantities related to  $^{157}\text{Gd}$  and  $^{158}\text{Gd}$ , respectively, in the above equations.

## 4 Analysis of the data

We use data from five new samples [15] recently taken from reactor zones (hereafter called RZs) 10 and 13, which are located deep underground, 150{250 m below the surface, in contrast to the other RZs 1-9 and RZ 15, which are located near the surface. The use of samples from deep-lying RZs is important, because it minimizes contamination from in-flow of isotopes from the outside after the cessation of reactor operation.

It is obvious that any geological alteration of the reactor zones would reduce the quality of the isotopic data. Because the surface above the RZs is today partly covered with a layer enriched in rare-earth elements, in-flow of non-radiogenic components into the reactors might have considerably perturbed the isotopic compositions originating from the fission events two billion years ago. This possibility constitutes a major risk factor for natural contamination even if the present surface composition has existed only during a relatively short time period compared to the time that has elapsed since the cessation of the reactor fission phase. This geological observation suggests that we as a precautionary measure, to keep the contamination to a minimum, collect samples from deep-lying RZs. The quality of our new data obtained in this way is, for example, demonstrated by a much smaller scatter of the values we obtained for  $^{149}\text{Sm}$  compared to what was obtained in Ref. [13] from earlier samples taken from RZs 1-9.

### 4.1 Sm data

Table 2 shows measured and calculated results for the five samples labeled in the first row. The first four samples were taken from RZ 10, whereas the last sample was taken from RZ 13. Measurement errors are given in Ref. [15]. Because they are mostly below the level of percent they are negligible in our analysis. More details on this question will be reported elsewhere. The last row shows  $^{149}\text{Sm}$  calculated as described in Subsection 3.1. The result can be represented by

$$^{149}\text{Sm} = 91 \pm 6 \text{ kb}; \quad (25)$$

We then use Fig. 1 to estimate  $E_r = E_r - E_{r0}$ , for the assumed temperatures, with the results shown in Fig. 4.

Note that for the temperature range of interest there are two solutions for  $E_r$  for a given set of  $^{149}\text{Sm}$  and  $T$ . The right-branch solution in Fig. 1 passes through the area that covers  $E_r = 0$  whereas the left-branch solution extends to the far-negative region of  $E_r$ . We reject the latter.

Because of the strong temperature-dependence of the neutron-capture cross section of  $^{176}\text{Lu}$  most estimates of the reactor temperature have been based on observed isotopic ratios of  $^{176}\text{Lu} = ^{175}\text{Lu}$  [15,16]. These observations suggest a reactor temperature range 220{360 C. However, some data show a temperature that is higher than 1000 C, indicating a limitation of the method. The discrepancy may arise because some amount of Lu may have moved inside the reactor, or the measured cross section may not be fully reliable above 500 C. However, since it seems plausible to expect a temperature range 200{400 C, we obtain

$$E_r = 4 \pm 16 \text{ meV}; \quad \text{for } T = 200\{400 \text{ C}; \quad (26)$$

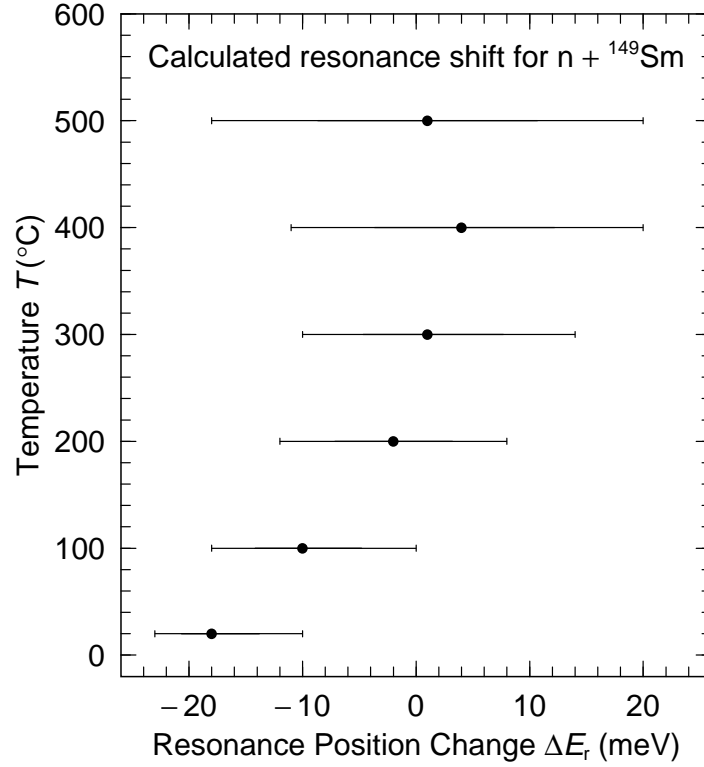


Figure 4: The ranges of  $E_r$ , represented by horizontal lines, calculated from Fig. 1 corresponding to the estimated cross section  $\hat{\sigma}_{149}$  given by (25) are shown for several choices of the temperature, namely  $T = 20; 100, 200, 300, 400, 500$  C .

where the standard deviation is determined from the lower and upper limits of the temperature.

In another approach, which is less direct, the oxygen isotopic compositions of clay minerals outside the reactor zone are measured. The results suggest a core temperature 300{350 C [17]. For this reason a narrower temperature range 300{400 C may also deserve serious consideration. For this more stringent temperature range we obtain

$$E_r = 5 \pm 16 \text{ meV}; \quad \text{for } T = 300\{400 \text{ C}; \quad (27)$$

which is nearly the same as obtained in (26). This indicates that the calculated  $E_r$  will not have to be revised, in case a somewhat different reactor temperature range is obtained in a refined future analysis.

As we alluded to before, one may suspect that the samples have been subjected to some post-reactor contamination. To obtain an estimate of this effect, we assume that a fraction of the natural abundance flowed into the reactor from the outside environment, contributing to the observed amount of Sm. We subtract this inflow from the now observed isotope abundances and apply the preceding analysis to the remainder to re-calculate  $\hat{\sigma}_{149}$ . As we can see in Table 3, the result is rather insensitive to as long as it stays around a few percent. This contamination range is suggested by our analysis of Gd below.

For  $\epsilon = 0.04$ , for example, we obtain

$$\hat{\sigma}_{149} = 99 \pm 10 \text{ kb} \quad (28)$$

	SF 84-1469	SF 84-1480	SF 84-1485	SF 84-1492	SD .37
0.00	85.6	96.5	83.8	99.0	89.5
0.01	86.4	100.2	85.6	100.7	90.4
0.02	87.1	104.3	87.4	102.4	91.3
0.03	87.8	108.6	89.3	104.2	92.2
0.04	88.6	113.4	91.2	106.0	93.2

Table 3: Estimated cross sections  $\sigma_{149}$  (kb) for five values of the post-reactor contamination for five samples.

instead of (25), from which follows

$$E_r = 2 \pm 14 \text{ meV}; \quad (29)$$

for either of the temperature ranges  $200\{400$  C and  $300\{400$  C. Although the result (28) seems worse than (25), the result (29) for  $E_r$  puts an even stronger limit on its time-variation than (26), because the curves corresponding to different temperatures in Fig. 1 happen to all intersect near  $E_r = 0$ . Therefore we can conclude that our Sm results are quite insensitive to the amount of contamination, as long as the amount is consistent with the Gd data, that is we assume a contamination of only a few percent.

## 4.2 Gd data

In analogy with our studies of the Sm isotopic compositions and estimates of neutron-capture cross sections tabulated in Table 2 we now study the measured Gd isotopic compositions in the Oklo RZs, which are tabulated in Table 4. By use of the formalism developed in Section 3.2 we obtain the estimates for the neutron-capture cross sections listed in the bottom two lines of Table 4. We find that the resonance-position change  $E_r$  deduced from the cross sections in Table 4 are generally significantly different from zero in contrast to what was indicated by the Sm results. It is therefore natural to investigate if the effect of contamination here, for Gd, plays a more crucial role than for Sm, which we found was relatively insensitive to modest contaminations. For Gd we divide the five samples into two different classes, which are presented separately in Tables 5 and 6. The samples SF 84-1469 and SF 84-1492 presented in Table 5 are characterized by much smaller abundances of  $^{157}\text{Gd}$  than are the other three samples presented in Table 6.

We assume that for each sample the unknown contamination parameter is the same for  $^{155}\text{Gd}$  and  $^{157}\text{Gd}$ , and investigate if there is any  $E_r$  for which we obtain the same  $E_r$  for both isotopes. For the sample SD .37 we have in Fig. 5 plotted  $E_r(\epsilon)$  determined in the following way. The neutron-capture cross sections  $\sigma_{155}$  and  $\sigma_{157}$  corresponding to the observed isotopic distributions with the assumed contamination removed, are calculated. The resonance-position changes corresponding to these cross sections are then obtained for the assumed reactor temperature limits from the appropriate curves in Figs. 2 and 3.

	Sample				
	SF 84-1469	SF 84-1480	SF 84-1485	SF 84-1492	SD 37
$N_{155}(t_1) (\%)$	0.5006	0.4608	0.6065	0.3899	0.5915
$N_{156}(t_1) (\%)$	30.03	29.46	30.79	29.90	30.37
$N_{157}(t_1) (\%)$	0.0418	0.2641	0.1921	0.0505	0.1881
$N_{158}(t_1) (\%)$	23.66	25.07	26.52	23.68	17.31
$N_{160}(t_1) (\%)$	11.21	12.24	12.93	10.95	6.1030
$\hat{\sigma}_{155} (kb)$	30.9	16.8	17.8	36.7	26.3
$\hat{\sigma}_{157} (kb)$	83.3	8.0	14.3	73.7	23.3

Table 4: Measured isotopic ratios for Gd for five samples and the corresponding, calculated cross sections  $\hat{\sigma}_{155}$  and  $\hat{\sigma}_{157}$ .

For the assumed temperature range 200{400 C, the bands for  $^{155}\text{Gd}$  and  $^{157}\text{Gd}$  do intersect each other for  $\beta$  in the range 0.036{0.040, yielding the range -26 meV to +9 meV for  $E_r$ . Similar results are obtained for the other samples except for SF 84-1492 for which no reasonable solution is obtained.

In Fig. 6 we summarize the ranges of  $\beta$  and  $E_r$  obtained for the four samples. It is remarkable to find that, with the exception of SF 84-1485, the obtained values of  $E_r$  are consistent with the Sm result (26). The presence of contamination is clearly indicated and its magnitude is also consistent with the Sm data.

As for SF 84-1485 and SF 84-1492, one may suspect non-uniform contamination inside the reactor core or some other type of error. This suggests that more stringent limits on the variation of  $E_r$  would be achieved by collecting additional samples. It might be argued that assuming a common value of the contamination parameter  $\beta$  for the two isotopes is not well founded. However, it is the most simple assumption, and with this

	SF 84-1469		SF 84-1492	
	$\hat{\sigma}_{155}$ (kb)	$\hat{\sigma}_{157}$ (kb)	$\hat{\sigma}_{155}$ (kb)	$\hat{\sigma}_{157}$ (kb)
0.000	30.9	83.3	36.7	73.7
0.001	31.4	102.9	37.4	87.2
0.002	31.9	134.7	38.1	106.6
0.003	32.3	195.0	38.8	137.1

Table 5: Calculated cross sections  $\hat{\sigma}_{155}$  and  $\hat{\sigma}_{157}$  for two samples and four values of the post-reactor contamination  $\beta$ .

	SF 84-1480		SF 84-1485		SD 37	
	$\hat{\sigma}_{155}$ (kb)	$\hat{\sigma}_{157}$ (kb)	$\hat{\sigma}_{155}$ (kb)	$\hat{\sigma}_{157}$ (kb)	$\hat{\sigma}_{155}$ (kb)	$\hat{\sigma}_{157}$ (kb)
0.00	16.8	8.0	17.8	14.3	26.3	23.3
0.01	20.2	11.1	20.6	26.4	28.1	29.9
0.02	25.4	20.6	24.4	236.9	30.2	42.0
0.03	34.4	227.1	30.1		32.7	70.9
0.04	53.5		39.2		35.6	235.3

Table 6: Calculated cross sections  $\hat{\sigma}_{155}$  and  $\hat{\sigma}_{157}$  for three samples and five values of the post-reactor contamination  $\beta$ . Dash (|) entries are given when the calculated cross sections are much larger than any of those occurring in Fig. 3.

assumption the  $S_m$  and  $G_d$  results are entirely consistent with each other, both for the contamination parameter  $\beta$  and for the resonance-position change  $E_r$  for which the  $S_m$  and  $G_d$  mutually support the conclusion  $E_r = 0$ .

## 5 Relation of the resonance-position change to the variation of the coupling constants

As was suggested in Section 1, a change  $\delta s$  of the strong coupling constant  $s$  corresponds to a change  $\delta M$  of a mass scale  $M$

$$\frac{\delta M}{M} = -\frac{\delta s}{s} \quad (30)$$

Shlyakhter specifically chose  $M = V_0 = 40 \text{ MeV}$ , the depth of the 1-particle potential of the nuclear force. For this choice one expects that

$$E_r = M \quad (31)$$

would result in

$$E_r = -\frac{\delta s}{s} M = M \frac{\delta s}{s} \quad (32)$$

This implies that when one relates the fractional change  $\delta s/s$  to  $E_r$  then it is inversely proportional to  $M$ .

With these assumptions (26) gives

$$\frac{\delta s}{s} = 2.5 \cdot 10^{-19} \text{ y}^{-1} \quad (33)$$

One may argue instead that the resonance in question is an excited state in a many-particle system and therefore unrelated to the model assumption of a 1-particle potential.

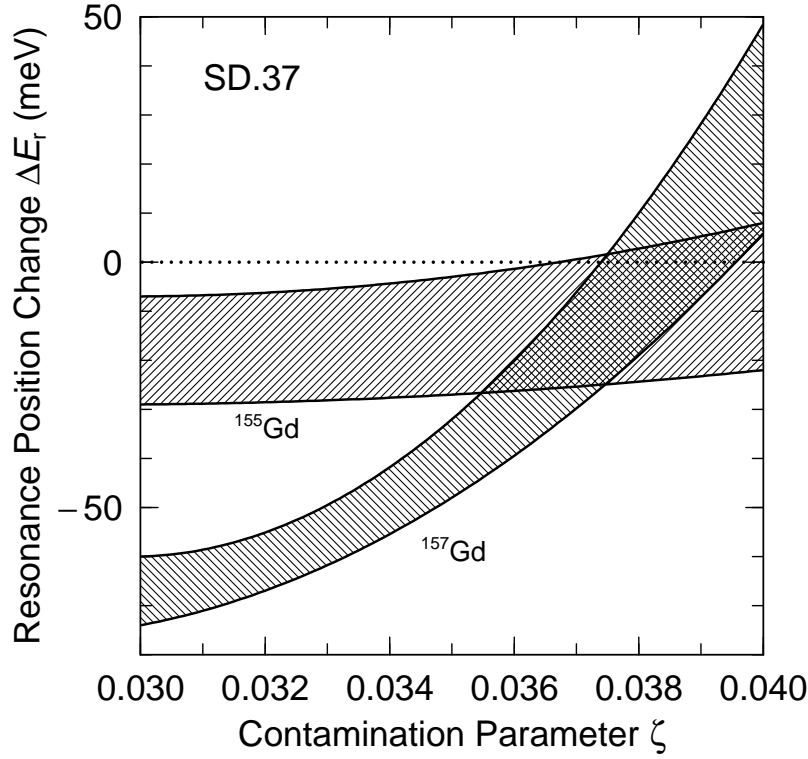


Figure 5: For the sample SD.37 we plot the resonance-position change  $\Delta E_r$  for  $^{155}\text{Gd}$  and  $^{157}\text{Gd}$  versus the contamination parameter  $\zeta$ , the ratio of the post-reactor contamination to the natural abundance. The two bands show the range of  $\Delta E_r$  for the temperature range 200{400 C, with the lower bound of each band corresponding to  $T = 200$  C and the upper bound to  $T = 400$  C. From the location of the overlap region of the two bands we deduce that the contamination parameter  $\zeta$  is in the range 0.0355 to 0.0403 and that the resonance-position change  $\Delta E_r$  is in the range -26 meV to +9 meV.

Then the relevant energy scale should be a neutron separation energy  $V_n \approx 8$  MeV. According to the previous argument we then expect

$$\frac{j-s}{j} \approx 1.3 \cdot 10^{-18} \text{ y}^{-1} : \quad (34)$$

On the other hand, Damour and Dyson showed that the Coulomb energy should be of significant magnitude in medium-heavy nuclei like Sm. Assuming that only the electromagnetic interaction is responsible for  $\Delta E_r$ , they obtained the estimate  $M \approx 1$  MeV in (30) with  $s$  replaced by  $r$ . Equations (33) or (34) are then replaced by

$$\frac{j-r}{j} \approx 1.0 \cdot 10^{-17} \text{ y}^{-1} : \quad (35)$$

which is about five times more stringent than in [13].

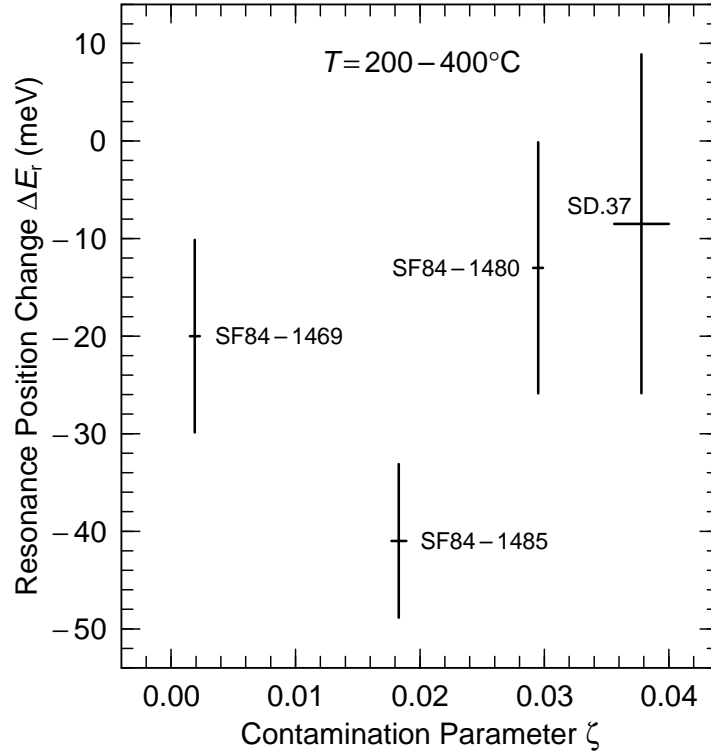


Figure 6: Summary of the ranges of  $E_r$  and  $\zeta$  estimated from Gd data from four samples, for the assumed temperature range  $T = 200\{400$  C .

## 6 Summary

We have examined in detail Shlyakhter's derivation of the upper bound on the shift with time of the resonance energy of  $^{149}\text{Sm}$ , given more complete details of the method, and applied it to new, carefully collected samples from deep-lying Oklo reactor zones. We reached the conclusion  $|E_r| < 16$  meV, from which we derived  $j_s = s < 2.5 \cdot 10^{19} \text{ y}^{-1}$  or  $1.3 \cdot 10^{18} \text{ y}^{-1}$  depending which mass-scale assumption is most closely connected to the strong-interaction coupling constant. For the electromagnetic coupling constant we obtained  $j_e = < 1.0 \cdot 10^{17} \text{ y}^{-1}$ . The surprising agreement between the result (26) and Shlyakhter's original result is probably somewhat accidental, since he in early years probably had access to few uncontaminated samples and since he also assumed the unrealistically low temperature  $T = 20$  C .

The cross section deduced from the 15 samples analyzed in Ref. [13] is  $\sigma_{149} = 73 \pm 9$  kb (one standard deviation; Ref. [13] gives an error corresponding to the outer limits of the cross sections obtained from the 15 samples). The lower cross section  $\sigma_{149}$  and its less stringent error limit were probably obtained because contamination was not considered in the analysis. However, we observe that the lower limit  $\sim 120$  meV for their estimate  $120 \text{ meV} < E_r < 90 \text{ meV}$  comes from the left-branch solutions mentioned above. If only right-branch solutions are considered, then their result for the resonance-position change is  $E_r = 41 \pm 29$  meV for our assumed temperature range  $200\{400$  C .

We also studied the isotopic composition of Gd in Oklo, to look, for the first time, for a possible time-variation in the position of the low-lying resonances in  $^{155,157}\text{Gd}$  and

a corresponding time-variation of the strong-interaction coupling constant. We used the same methodology as in the studies of Sm. In the Gd analysis it was crucial to determine the amount of post-reactor contamination, in contrast to the case in the Sm analysis. The results of the Gd studies confirm and reinforce the conclusions based on the  $^{149}\text{Sm}$  data.

Because Shlyakhter only presented very limited details about his derivation of the upper bound on the shift with time of the resonance energy in  $^{149}\text{Sm}$ , his very low bounds on the time-variability of the fundamental constants were perhaps not always taken very seriously. We hope that we have shown with our detailed analysis here, that the constraints from the Oklo phenomenon should be considered to be quite realistic upper bounds on the time-variability of the fundamental constants. This result should provide valuable guidance in the search for viable unification models.

The result obtained here, that the upper bounds on the rate-of-change of the fundamental constants are much lower than the value  $10^{-10} \text{ y}^{-1}$  expected naturally in terms of the present age of the universe is likely linked to the cosmological constant problem, suggesting the presence of a small but nonzero  $\Lambda$  [18,21]. One of the unique features of the approach in this paper, in contrast to the cosmological studies of the time-variation of the fundamental constants, is that we probe the time  $\sim 2 \times 10^9 \text{ y}$  ago. This is somewhat less distant than some cosmological phenomena considered so far, which have typical time scales of  $10^{10} \text{ y}$  [3,5,8]. The different time scales of the studies may be useful in trying to understand the recent finding that the fine-structure constant seems to exhibit a complicated time dependence [22].

We thank John Barrow for giving us important insight to the whole subject through his book [23] and for providing access to Ref. [7]. We are grateful to Thibault Damour for pointing out to us the importance of the effective cross section in the analysis of the Oklo phenomena.

The present work was partially supported by the REIMEIR research Resources of Japan Atomic Energy Research Institute and by the US Department of Energy.

## Appendix

### A Numerical details

The integral

$$I_c = \int_0^{Z-1} dE \frac{P}{E} \exp(-E/T) \frac{E}{(E - E_r)^2 + \frac{\Gamma^2}{4}} \quad (\text{A } 1)$$

occurring in Eq. (8) has to be evaluated by numerical quadrature. So that we can use Gauss-Laguerre integration we make the substitution  $x = E/T$  and obtain

$$I_c = T \int_0^{Z-1} dx \frac{P}{xT} \exp(-x) \frac{E}{(xT - E_r)^2 + \frac{\Gamma^2}{4}} = T \int_0^{Z-1} dx \exp(-x) f_1(x) : \quad (\text{A } 2)$$

where

$$f_1(x) = \frac{P}{xT} \frac{E}{(xT - E_r)^2 + \frac{\Gamma^2}{4}} : \quad (\text{A } 3)$$

Because  $f_1$  has a maximum at

$$x_{\max} = \frac{E_r + \sqrt{4E_r^2 + 3(\tau_{\text{tot}}=2)^2}}{4T}; \quad (\text{A.4})$$

it is necessary to divide the integration interval into two parts to achieve satisfactory numerical accuracy. The first part of the integration should include the maximum of the function  $f_1$  and thus go from 0 to  $x_d$  where

$$x_d = 2x_{\max} \quad (\text{A.5})$$

is a suitable choice. However, the numerical results are very stable to reasonable variations of the choice of  $x_d$ . Thus we rewrite

$$I_c = \int_0^{x_d} dx \frac{1}{xT \exp(-x)} \frac{E}{(xT - E_r)^2 + \tau_{\text{tot}}^2=4} + \int_{x_d}^{\infty} dx \frac{1}{xT \exp(-x)} \frac{E}{(xT - E_r)^2 + \tau_{\text{tot}}^2=4} \quad (\text{A.6})$$

So that we can use Gauss-Laguerre integration on the latter integral we substitute  $y = x - x_d$  and obtain

$$I_c = \int_0^{x_d} dx \frac{1}{xT \exp(-x)} \frac{E}{(xT - E_r)^2 + \tau_{\text{tot}}^2=4} + \int_0^{\infty} dy \frac{1}{(y + x_d)T \exp(-x_d) \exp(-y)} \frac{E}{((y + x_d)T - E_r)^2 + \tau_{\text{tot}}^2=4} \quad (\text{A.7})$$

The first integral can now be calculated using Gauss-Legendre integration and the last integral can be calculated by Gauss-Laguerre integration. Thus we obtain for the numerical evaluation of Eq. A.1

$$I_c = \sum_{i=1}^{N^G} \frac{1}{N^G} F^G(x_i^G) + \exp(-x_d) \sum_{i=1}^{N^L} \frac{1}{N^L} F^L(y_i^L) \quad (\text{A.8})$$

where the superscripts G and L indicate Gauss-Legendre and Gauss-Laguerre integration, respectively, and where

$$F^G(x) = \frac{1}{xT \exp(-x)} \frac{E}{(xT - E_r)^2 + \tau_{\text{tot}}^2=4} \quad (\text{A.9})$$

and

$$F^L(y) = \frac{1}{(y + x_d)T} \frac{E}{((y + x_d)T - E_r)^2 + \tau_{\text{tot}}^2=4} \quad (\text{A.10})$$

Note that the exponential term is retained in  $F^G$  but not in  $F^L$ .

## References

- 1) Y. Fujii, Oklo Phenomenon Revisited | Strong Interaction Coupling Constant Time-Dependent? in Proceedings of International Workshop on Gravitation and Astrophysics, ICRR, University of Tokyo, 17-19 November, 1997.
- 2) P. A. M. Dirac, Proc. Roy. Soc. A 165 (1938) 199.
- 3) F. Hoyle, Galaxies, Nuclei and Quasars, Heinemann (London), 1965.
- 4) F. J. Dyson, Phys. Rev. Lett. 19 (1967) 1291.
- 5) P. C. W. Davies, J. Phys. A 5 (1972) 1296.
- 6) A. I. Shlyakhter, Nature 264 (1976) 340.
- 7) A. I. Shlyakhter, ATOMKIREport A/1 (1983), unpublished.
- 8) L. L. Cowie and A. Songalia, Ap. J. 453 (1995) 596.
- 9) A. Godone, et al, Phys. Rev. Lett. 71 (1993) 2364.
- 10) R. W. Hellings, et al, Phys. Rev. Lett. 51 (1983) 1609.
- 11) See, for example, The Oklo Phenomenon, Proc. of a Symposium, Libreville, June, 1975 (IAEA, Vienna, 1975).
- 12) Natural Fission Reactors, Proc. of a meeting on natural fission reactor, Paris, France, December, 1977 (IAEA, Vienna, 1978).
- 13) T. Damour and F. Dyson, Nucl. Phys. B 480 (1996) 37.
- 14) M. Lucas, R. Hagemann, R. Naudet, C. Renson and C. Chevalier, Natural Fission Reactors, Proc. of a meeting on natural fission reactor, Paris, France, December, 1977 (IAEA, Vienna, 1978) p. 407.
- 15) H. Hidaka and P. Holliger, Geochim. Cosmochim. Acta 62 (1998), 89.
- 16) P. Holliger and C. Deviller, Earth Planet. Sci. Lett. 52 (1981), 76.
- 17) F. Gauthier-Lafaye, F. Weber and H. Ohmoto, Econ. Geol. 84 (1989) 2286.
- 18) Y. Fujii and T. Nishioka, Phys. Rev. D 42 (1990) 361.
- 19) Y. Fujii, M. Omote and T. Nishioka, Prog. Theor. Phys. 92 (1994), 521.
- 20) Y. Fujii, Astrop. Phys. 5 (1996) 133.
- 21) Y. Fujii, and a new type of dissipative structure, delivered at XXXIIIrd Rencontres de Moriond, Fundamental Parameters in Cosmology (Les Arcs, France, January 17-24, 1998) and papers cited therein (Los Alamos e-Print Archive gr-qc/9806089).
- 22) J. K. Webb, V. V. Fainbaum, C. W. Churchill, M. J. Drinkwater and J. D. Barrow, Evidence for time variation of the fine structure constant, preprint, 1998 (Los Alamos e-Print Archive astro-ph/9803165).
- 23) J. D. Barrow and F. J. Tipler, The Anthropic Cosmological Principle, Clarendon Press, Oxford, 1986.